

Ethereal Solvation of Lithium Hexamethyldisilazide: Unexpected Relationships of Solvation Number, Solvation Energy, and Aggregation State

Brett L. Lucht and David B. Collum*

Contribution from the Department of Chemistry, Baker Laboratory, Cornell University, Ithaca, New York 14853-1301

Received May 26, 1995[⊗]

Abstract: ^6Li , ^{15}N , and ^{13}C NMR spectroscopic studies of ^6Li – ^{15}N labeled lithium hexamethyldisilazide ($[^6\text{Li},^{15}\text{N}]$ -LiHMDS) are reported. Mono-, di-, and mixed-solvated dimers are characterized in the limit of slow solvent exchange for a variety of ethereal ligands including the following: tetrahydrofuran (THF), 2-methyltetrahydrofuran (2-MeTHF), 2,2-dimethyltetrahydrofuran (2,2-Me₂THF), diethyl ether (Et₂O), *tert*-butyl methyl ether (*t*-BuOMe), *n*-butyl methyl ether (*n*-BuOMe), tetrahydropyran (THP), methyl isopropyl ether (*i*-PrOMe), and trimethylene oxide (oxetane). The ligand exchange is too fast to observe bound and free diisopropyl ether (*i*-Pr₂O), *tert*-amyl methyl ether (Me₂(Et)COMe), and 2,2,5,5-tetramethyltetrahydrofuran (2,2,5,5-Me₄THF). Exclusively dissociative ligand substitutions occur at low ligand concentrations for all ligands except oxetane. Relative free energies and enthalpies of LiHMDS dimer solvation determined for eight ethereal ligands show an approximate inverse correlation of binding energy and ligand steric demand. Mixed solvation is found to be non-cooperative showing there exists little communication between the two lithium sites on the dimer. The different ethereal solvents display a widely varying propensity to cause formation of LiHMDS monomer. The often-cited correlation of reduced aggregation state with increasing strength of the lithium–solvent interaction receives no support whatsoever. The measured free energies of aggregation display a considerable solvent dependence that is traced to solvent-independent enthalpies of aggregation and solvent-dependent entropies of aggregation. LiHMDS monomer solvation numbers derive from solvent-concentration-dependent monomer:dimer proportions. Moderately hindered ethereal solvents afford LiHMDS monomers in trisolvated forms ((Me₃Si)₂NLiS₃) whereas THF and oxetane appear to afford considerable concentrations of five-coordinate tetrasolvates ((Me₃Si)₂NLiS₄). The complex relationship between solvation energy and observable aggregation state is discussed in light of solvent–amide and solvent–solvent interactions on both the monomer and the dimer, the combined contributions of solvation enthalpy and entropy, and the complicating intervention of variable solvation numbers.

Introduction

One of the most universally accepted dictums to emerge from organolithium chemistry is that strong donor solvents promote dissociation of the self-associated aggregates.^{1–3} While it certainly seems logical that solvation energy is necessary to compensate for the loss of aggregation energy, direct determinations of absolute or relative energies of lithium ion solvation are quite rare.^{4,5} Calorimetric studies have very rarely deconvoluted the contributions of changes in aggregation and solvation number to the measured enthalpies of solvation.⁵ Extrapolation of complexation enthalpies for non-lithium Lewis acids (e.g.

Gutmann donor numbers)⁶ to lithium ion in its highly variable environments is a questionable practice. The thousands of empirically observed solvent effects on organolithium structure and reactivity (including solvent-dependent deaggregations themselves) appear to offer evidence of relative solvation energies. However, this evidence, no matter how logical and compelling it may seem, is circumstantial and potentially grossly misleading. The powerful computational methods may offer the most reliable probe of solvation energy,⁷ but they still require experimental verification. Thus, it would be very difficult, for example, to document with unassailable experimental data the widely held notion that THF is generally superior to Et₂O as a ligand for the lithium ion.⁸

[⊗] Abstract published in *Advance ACS Abstracts*, August 15, 1995.

(1) Seebach, D. *Angew. Chem., Int. Ed. Engl.* **1988**, *27*, 1624. *Ions and Ion Pairs in Organic Reactions*; Swarc, M., Ed.; Wiley: New York, 1972; Vols. 1 and 2. Weiss, E. *Angew. Chem., Int. Ed. Engl.* **1993**, *32*, 1501. Jackman, L. M.; Bortiatynski, J. In *Advances in Carbanion Chemistry*; JAI: New York, 1992; Vol. 1, pp 45–87. Wardell, J. L. In *Comprehensive Organometallic Chemistry*; Wilkinson, G., Stone, F. G. A., Abels, F. W., Eds.; Pergamon: New York, 1982; Vol. 1, Chapter 2.

(2) Reviews of structural studies of *N*-lithiated species: Gregory, K.; Schleyer, P. v. R.; Snaith, R. *Adv. Inorg. Chem.* **1991**, *37*, 47. Mulvey, R. E. *Chem. Soc. Rev.* **1991**, *20*, 167. Collum, D. B. *Acc. Chem. Res.* **1993**, *26*, 227.

(3) Reviews on the reactivity of lithium amides: d'Angelo, J. *Tetrahedron* **1976**, *32*, 2979. Heathcock, C. H. In *Comprehensive Carbanion Chemistry*; Buncl, E., Durst, T., Eds.; Elsevier: New York, 1980; Vol. B, Chapter 4. Cox, P. J.; Simpkins, N. S. *Tetrahedron: Asymmetry* **1991**, *2*, 1. *Asymmetric Synthesis*; Morrison, J. D., Ed.; Academic Press: New York, 1983; Vols. 2 and 3. Evans, D. A. In *Asymmetric Synthesis*; Morrison, J. D., Ed.; Academic Press: New York, 1983; Vol. 3, Chapter 1. Snieckus, V. *Chem. Rev.* **1990**, *90*, 879.

(4) Burgess, J. *Metal Ions in Solution*; Wiley: New York, 1978. *Chemistry of Nonaqueous Solutions*; Mamantov, G., Popov, A. I., Eds.; VCH: New York, 1994.

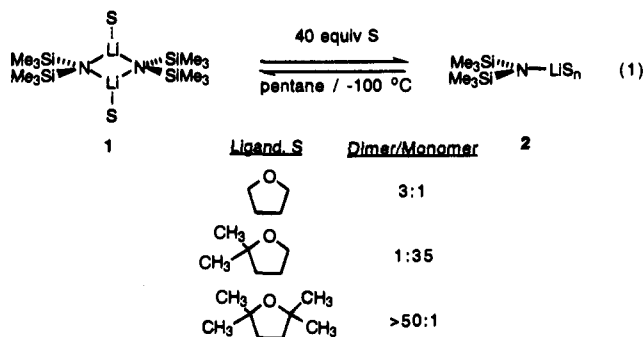
(5) Kminek, I.; Kaspar, M.; Tvekoval, J. *Collect. Czech. Chem. Commun.* **1981**, 1124, 1132. Arnett, E. M.; Moe, K. D. *J. Am. Chem. Soc.* **1991**, *113*, 7288. Arnett, E. M.; Fisher, F. J.; Nichols, M. A.; Ribeiro, A. A. *J. Am. Chem. Soc.* **1990**, *112*, 801. Quirk, R. P.; McFay, D. *J. Polym. Sci., Polym. Chem. Ed.* **1986**, *24*, 827. Quirk, R. P.; McFay, D. *J. Polym. Sci., Polym. Chem. Ed.* **1981**, *19*, 1445. Beak, P.; Siegel, B. *J. Am. Chem. Soc.* **1974**, *96*, 6803. Quirk, R. P.; Kester, D. E.; Delaney, R. D. *J. Organomet. Chem.* **1973**, *59*, 45. Quirk, R. P.; Kester, D. E. *J. Organomet. Chem.* **1974**, *72*, C23. Quirk, R. P.; McFay, D. *Makromol. Chem., Rapid Commun.* **1980**, *102*, 5741. See also: Heinzer, J.; Oth, J. F. M.; Seebach, D. *Helv. Chim. Acta* **1985**, *68*, 1848.

(6) Gutmann, V. *The Donor–Acceptor Approach to Molecular Interactions*; Plenum: New York, 1978.

(7) Kaufmann, E.; Gose, J.; Schleyer, P. v. R. *Organometallics* **1989**, *8*, 2577.

The putative correlation of reduced aggregation state with high solvation energy has recently been challenged. For example, the demonstrably powerful ligand hexamethylphosphoramide (HMPA) has been shown most convincingly by Reich and co-workers to cause dissociation of LiX-based aggregates to ion pairs in many cases.⁹ However, HMPA profoundly influences lithium amide solution structures *without significantly altering the overall aggregation state*.^{10,11} $R_2NLi-LiX$ mixed aggregation was shown to be either promoted or retarded by HMPA, depending upon the substituents on the lithium dialkylamide and LiX salt.^{12,13} Jackman and Chen found that dimeric lithium phenolates in THF solution are driven to tetramers with added HMPA.¹⁴ Addition of cryptands to lithiated hydrazones affords triple ions of the general structure $[R_2Li]^{-}/Li^+Li-L$ rather than the anticipated simple ion pairs.¹⁵ Turning to the most commonly employed bidentate ligand *N,N,N',N'*-tetramethylethylenediamine (TMEDA), a detailed analysis of the literature suggested that the strength of the TMEDA-lithium interaction may be highly sensitive to the structure of the organolithium and that observable TMEDA-mediated deaggregations do not necessarily coincide with those instances where the metal-ligand interaction is strong.¹⁶ For example, TMEDA is particularly efficient relative to THF at mediating deaggregation of lithium hexamethyldisilazide (LiHMDS), yet is unable to compete with THF for coordination to LiHMDS.¹⁷

The work described herein may be best introduced by jumping ahead to the poignant solvent-dependent deaggregation of LiHMDS depicted in eq 1. If we accept the notion that



increasing steric demands of the ligand should cause a net destabilization of the metal-ligand interaction,¹⁸ it would appear that the relationship between solvation energy and LiHMDS

(8) One could best make such a case with the following: Lewis, H. L.; Brown, T. L. *J. Am. Chem. Soc.* **1970**, *92*, 4664. Sergutin, V. M.; Zgonnik, V. N.; Kalninsk, K. K. *J. Organomet. Chem.* **1979**, *170*, 151. Quirk, R. P.; Kester, D. E. *J. Organomet. Chem.* **1977**, *127*, 111.

(9) Leading references: Reich, H. J.; Borst, J. P.; Dykstra, R. R. *Organometallics* **1994**, *13*, 1.

(10) Romesberg, F. E.; Gilchrist, J. H.; Harrison, A. T.; Fuller, D. J.; Collum, D. B. *J. Am. Chem. Soc.* **1991**, *113*, 5751.

(11) Romesberg, F. E.; Bernstein, M. P.; Fuller, D. J.; Harrison, A. T.; Collum, D. B. *J. Am. Chem. Soc.* **1993**, *115*, 3475.

(12) Romesberg, F. E.; Collum, D. B. *J. Am. Chem. Soc.* **1994**, *116*, 9198.

(13) HMPA precludes formation of MeLi-LiCl mixed aggregates: Reich, H. J.; Borst, J. P.; Dykstra, R. R.; Green, D. P. *J. Am. Chem. Soc.* **1993**, *115*, 8728.

(14) Jackman, L. M.; Chen, X. *J. Am. Chem. Soc.* **1992**, *114*, 403.

(15) Galiano-Roth, A. S.; Collum, D. B. *J. Am. Chem. Soc.* **1988**, *110*, 3546.

(16) Collum, D. B. *Acc. Chem. Res.* **1992**, *25*, 448.

(17) Bernstein, M. A.; Lucht, B. L.; Collum, D. B. Unpublished. For a preliminary description, see ref 16.

(18) For an early suggestion that steric effects are major determinants of solvation, see: Settle, F. A.; Haggerty, M.; Eastham, J. F. *J. Am. Chem. Soc.* **1964**, *86*, 2076.

aggregation state is not simple. We will describe a combination of NMR spectroscopic and semiempirical (MNDO) computational studies of dimeric and monomeric LiHMDS (**1** and **2**, respectively) solvated by a wide range of ethereal ligands.¹⁹⁻²¹ We will demonstrate the following: (1) Mono- and disolvated dimers are observable in the slow exchange limit for all but the most hindered ethereal ligands.²² Ligand substitution of the disolvated dimers occurs by dissociative pathways at low ligand concentrations for most ethereal solvents. (2) The relative free energies of dimer **1** and monomer **2** ($\Delta\Delta G^\circ_{\text{agg}}$) do not correlate with free energies of dimer solvation. The solvent dependence of $\Delta\Delta G^\circ_{\text{agg}}$ stems almost entirely from the solvent-dependent entropies ($\Delta\Delta S^\circ_{\text{agg}}$) rather than enthalpies ($\Delta\Delta H^\circ_{\text{agg}}$).²³ (3) Monomers are routinely trisolvated rather than disolvated, while oxetane and THF appear to afford mixtures of trisolvated monomers and *five-coordinate tetrasolvated* monomers. (4) Overall, the results highlight previous concerns¹⁶ that the often-cited relationships between solvation, aggregation, and reactivity require reevaluation.

Results

Structure Assignments of LiHMDS Ethereal Solvates.

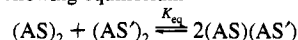
The protocols for lithium amide solution structure determination using ^6Li - ^{15}N doubly labeled substrate are now well established.²⁴⁻²⁶ Applications of these methods to the characterization of monosolvated dimers, disolvated dimers, monomers, and mixed-solvated dimers (**3a-1**, **1a-1**, **2a-1**, and **4a-n**; Tables 1 and 2) share many common features that are readily illustrated using THF as a case study. The majority of NMR spectra and a number of plots referred to throughout the manuscript are included as supporting information. ^6Li and ^{15}N NMR spectra recorded on 0.1 M solutions of $[^6\text{Li}, ^{15}\text{N}]\text{LiHMDS}$ in pentane show two ^6Li 1:2:1 triplets and two ^{15}N 1:2:3:2:1 quintets previously assigned as dimer **5** and higher oligomer **6** (Figure 1A).^{11,20} As noted previously by Kimura and Brown,²⁰ dimer **5** is essentially the only observable form in toluene. The

(19) For a preliminary communication describing a portion of this work, see: Lucht, B. L.; Collum, D. B. *J. Am. Chem. Soc.* **1994**, *116*, 6009.

(20) For the first detailed study of LiHMDS solution structure, see: Kimura, B. Y.; Brown, T. L. *J. Organomet. Chem.* **1971**, *26*, 57.

(21) For additional structural studies of LiHMDS, see: Wannagat, U. *Adv. Inorg. Chem. Radiochem.* **1964**, *6*, 237. Arnett, E. M.; Moe, K. D. *J. Am. Chem. Soc.* **1991**, *113*, 7288. Rogers, R. D.; Atwood, J. L.; Grüning, R. *J. Organomet. Chem.* **1978**, *157*, 229. Mootz, D.; Zinnius, A.; Böttcher, B. *Angew. Chem., Int. Ed. Engl.* **1969**, *8*, 378. Renaud, P.; Fox, M. A. *J. Am. Chem. Soc.* **1988**, *110*, 5702. Fjeldberg, T.; Lappert, M. F.; Thorne, A. J. *J. Mol. Struct.* **1984**, *125*, 265. Fjeldberg, T.; Hitchcock, P. B.; Lappert, M. F.; Thorne, A. J. *J. Chem. Soc., Chem. Commun.* **1984**, 822. Engelhardt, L. M.; May, A. S.; Raston, C. L.; White, A. H. *J. Chem. Soc., Dalton Trans.* **1983**, 1671. Williard, P. G.; Liu, Q.-Y.; Lochmann, L. *J. Am. Chem. Soc.* **1992**, *114*, 348. Lochmann, L.; Trekoval, J. *J. Organomet. Chem.* **1975**, *99*, 329. Williard, P. G.; Nichols, M. A. Unpublished. Atwood, J. L.; Lappert, M. F.; Leung, W.-P.; Zhang, H. Unpublished. Boche, G.; Langlotz, I.; Marsch, M.; Harms, K.; Frenking, G. *Angew. Chem., Int. Ed. Engl.* **1993**, *32*, 1171. Arnett, E. M.; Moe, K. D. *J. Am. Chem. Soc.* **1991**, *113*, 7068. See also ref 11.

(22) Given the following equilibrium



the solvation would be non-cooperative for $K_{\text{eq}} = 1.0$. While this holds for most solvent combinations, 2,2-Me₂THF/Et₂O and 2,2-Me₂THF/THF combinations afford slightly elevated concentrations of mixed solvate ($K_{\text{eq}} > 1.0$).

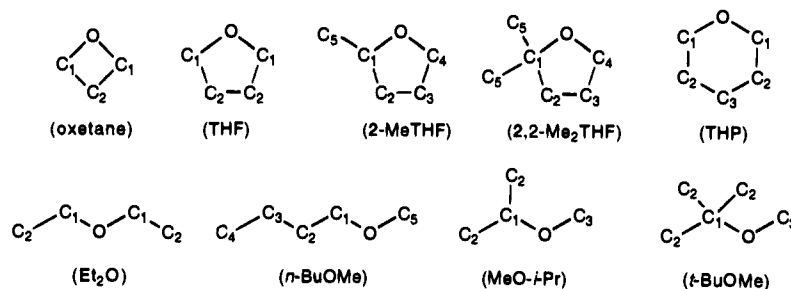
(23) For entropically dominated solvent-dependent ion pairing that may be related, see: Strong, J.; Tuttle, T. R., Jr. *J. Phys. Chem.* **1973**, *77*, 533.

(24) Collum, D. B. *Acc. Chem. Res.* **1993**, *26*, 227.

(25) Gilchrist, J. H.; Harrison, A. T.; Fuller, D. J.; Collum, D. B. *Magn. Reson. Chem.* **1992**, *30*, 855.

(26) Gilchrist, J. H.; Collum, D. B. *J. Am. Chem. Soc.* **1992**, *114*, 794.

Chart 1

Table 1. NMR Spectroscopic Data of [⁶Li,¹⁵N]LiHMDS Solvates^a

compd	⁶ Li δ (m, J _{N-Li})	¹⁵ N δ (m, J _{N-Li})	¹³ C ₁	¹³ C ₂	¹³ C ₃	¹³ C ₄	¹³ C ₅	¹³ C-Si
3a	1.42 (t,3.5); 1.78 (t,3.9)	41.7 (q,3.9)	68.2	24.7				5.3
3b	1.03 (t,3.4); 1.79 (t,3.6) ^b	42.2 (q,3.5) ^b	62.5	13.3				5.4
3c	1.74 (t,3.4); 0.77 (t,3.2) ^b	<i>c</i>	75.9 ^b	49.6 ^b	26.4 ^b			5.4 ^b
3d	1.11 (t,3.3); 1.39 (t,3.5)	43.9 (q,3.5)	76.1	31.9	21.1	68.1	25.0	5.5, 5.4, 5.3, 5.2 ^d
3e	1.03 (t,3.3); 0.42 (t,3.3)	42.8 (q,3.3)	83.3	37.3	25.0	67.7	27.5	5.5
3f,j,k	<i>e</i>	<i>e</i>	<i>e</i>					<i>e</i>
3g	1.33 (t,3.5); 1.81 (t,3.4)	43.5 (q,3.4)	68.6	25.2	22.0			5.4
3h	0.97 (t,3.6); 0.49 (t,3.3)	41.1 (q,3.4)	72.6	18.5	51.6			5.3
3i	1.76 (t,3.6); 1.20 (t,3.5)	43.9 (q,3.5)	72.1	29.2	18.6	14.4	56.5	5.3, 5.2 ^d
3l	1.62 (t,3.7); 1.06 (t,3.1)	<i>c</i>	73.5	<i>f</i>				5.4
1a	1.42 (t,3.5)	38.40 (q,3.5)	68.3	24.9				5.9
1b	1.21 (t,3.4)	38.23 (q,3.4)	60.4	12.4				5.9
1c	0.65 (t,3.3)	37.92 (q,3.2)	75.6	49.1 ^b	26.7 ^b			5.8 ^b
1d	1.26 (t,3.4)	38.09 (q,3.4) ^d	75.9	31.6	20.9	67.6	24.5	6.1 ^d
		37.98 (q,3.4) ^d						6.0 ^d
1e	0.91 (t,3.3)	37.74 (q,3.3)	83.4	37.7	25.3	68.3	28.1	5.9
1f	1.03 (t,3.3)	42.53 (q,3.2)	<i>e</i>					
1g	1.26 (t, 3.5)	38.41 (q,3.5)	68.6	25.2	22.1			5.9
1h	1.19 (t,3.2)	38.33 (q,3.3)	70.8	18.6	47.7			5.8
1i	1.25 (t,3.4)	38.52 (q,3.5)	72.3	32.3	19.7	14.4	58.3	5.8
1j	0.62 (t,3.3)	38.24 (q,3.3)	<i>e</i>					
1k	0.80 (t,3.3)	38.61 (q,3.3)	<i>e</i>					
1l	1.05 (t,3.5)	42.73 (q,3.5)	73.2	<i>f</i>				5.8
2a	0.24 (d,5.0)	41.2 (t,5.0)						
2b	1.02 (d,5.9)	48.8 (t,6.1)						
2c	0.29 (d,5.9)	50.7 (t,5.9)						
2d	0.84 (d,5.7)	48.8 (t,5.7)						
2e	0.33 (d,5.7)	49.4 (t,5.8)						
2f,k	<i>g</i>	<i>g</i>						
2g	0.01 (d,5.2)	45.6 (t,5.2)						
2h	0.77 (d,6.0)	50.3 (t,5.9)						
2i	0.78 (d,6.0)	49.0 (t,6.0)						
2j	0.51 (d,6.2)	47.7 (t,5.8)						
2l	-0.29 (d,5.0)	44.8 (t,5.0)						
	-0.36 (d,5.3)	45.2 (t,5.2)						

^a Spectra were recorded on 0.1 M solutions of LiHMDS at -100 °C in either pentane (⁶Li and ¹⁵N NMR spectra) or toluene-*d*₈ (¹³C NMR spectra). Coupling constants were measured after resolution enhancement. Multiplicities are denoted as follows: d = doublet, t = triplet, q = quintet. The chemical shifts are reported relative to 0.3 M ⁶LiCl/MeOH at -100 °C (0.0 ppm) and DMEA (25.7 ppm). Chemical shifts are dependent upon solvent concentration; chemical shifts of **1** and **3** are from samples with <5.0 equiv donor solvent and those of **2** are from samples containing 40 equiv of donor solvent. All *J* values are reported in hertz. Solvent carbon numbering is indicated in Chart 1. ^b Recorded at -120 °C. ^c Not recorded due to low solubility. ^d Multiple resonances are due to asymmetry imparted by solvent (see text). ^e Discrete resonances attributable to monosolvated and disolvated dimers are not observed due to rapid exchange with free solvent. ^f Resonance was not observed (possibly due to toluene resonances). ^g No monomer was observed.

distinction of dimers and higher oligomers is routinely achieved using inverse-detected ¹⁵N zero-quantum NMR spectroscopy.²⁶ The coupling in the F₁ (¹⁵N) dimension for one of the two unsolvated oligomers is consistent with a higher cyclic oligomer **6**. The species showing no coupling in F₁ is assigned as dimer **5**. With 0.3 equiv of added THF per lithium, the NMR spectra show two new ⁶Li triplets and a single new ¹⁵N quintet consistent with monosolvated dimer **3a** (Figure 1B). This is undoubtedly structurally related to a monosolvated LiHMDS dimer recently characterized crystallographically by Williard and Liu.²⁷ The ⁶Li-¹⁵N heteronuclear multiple quantum correlation (HMQC) spectrum²⁵ reveals resonance correlations con-

sistent with the assignment. With 0.7 equiv of THF per lithium, the ⁶Li and ¹⁵N NMR spectra display resonances corresponding to monosolvated dimer **3a** along with a new ⁶Li triplet and ¹⁵N quintet consistent with symmetric cyclic dimer **1a** (Figure 1C). As the [THF] exceeds 1.0 equiv per Li, the ⁶Li and ¹⁵N NMR spectra reveal dimer **1a** to be the sole observable structural form (Figure 1D). The ¹⁵N zero-quantum NMR spectrum reveals an absence of coupling in the ¹⁵N dimension, confirming the assignment of **1a** as a dimer rather than higher cyclic oligomer. At elevated [THF] (≥20 equiv per Li, 17% by volume), we observe new ⁶Li doublets and ¹⁵N triplets (1:1:1) characteristic of LiHMDS monomer **2a** (Figure 1E). Monomer **2a** is the dominant species in neat THF. ¹³C NMR

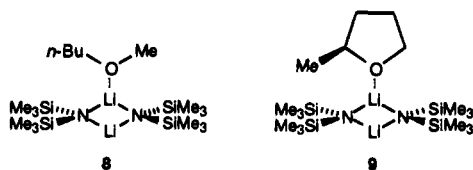
Table 2. NMR Spectroscopic Data of [⁶Li,¹⁵N]LiHMDS Mixed Solvated Dimers^a

compd	⁶ Li (m,J)	¹⁵ N (m,J)	C ₁ (S ₁)	C ₂ (S ₁)	C ₁ (S ₂)	C ₂ (S ₂)	C ₃ (S ₂)	C ₄ (S ₂)	C ₅ (S ₂)
4a	1.38 (t,3.3) 1.22 (t,3.4) ^b	38.29 (q,3.4) ^b	61.3	12.9	68.4	24.8			
4b	1.25 (t,3.5) 0.63 (t,3.5) ^b	37.91 (q,3.5) ^b	60.1 ^b	12.1 ^b	75.5 ^b	50.1 ^b	26.6 ^b		
4c	1.25 (t,3.5) 1.22 (t,3.5)	38.13 (q,3.5)	60.4	12.5	76.0	31.6	20.9	67.5	24.5
4d	1.26 (t,3.5) 0.84 (t,3.4)	37.82 (q,3.4)	60.0	12.1	83.4	37.7	25.3	68.3	28.1
4e	1.20 (t,3.2) 1.20 (t,3.2)	38.27 (q,3.3)	60.4	12.5	70.7	47.5	18.6		
4f	1.26 (t,3.4) 1.20 (t,3.4)	38.37 (q,3.5)	60.6	12.5	71.9	28.7	18.5	14.4	56.1
4g	1.27 (t,3.4) 1.18 (t,3.4)	38.28 (q,3.4)	61.0	12.7	68.8	26.6	22.1		
4h	^c								
4i	1.38 (t,3.0) 1.27 (t,3.3)	38.45 (q,3.1)	68.3	24.8	72.0	28.9	18.6	14.4	57.2
4j	1.37 (t,3.2) 1.20 (t,3.2)	38.33 (q,3.2)	^c						
4k	1.42 (t,3.3) 1.23 (t,3.4)	38.12 (q,3.4)	68.4	24.8	76.0	31.8	21.1	67.9	24.8
4l	1.42 (t,3.3) 0.92 (t,3.2)	37.95 (q,3.1)	68.2	24.9	79.8	37.9	26.2	66.9	28.1
4m	1.38 (t,3.3) 1.32 (t,3.4)	38.40 (q,3.3)	68.2	24.8	68.7	25.3	22.1		

^a Spectra were recorded on 0.1 M solutions of LiHMDS at -100 °C in either pentane (⁶Li and ¹⁵N NMR spectra) or toluene-*d*₈ (¹³C NMR spectra). Coupling constants were measured after resolution enhancement. Multiplicities are reported as follows: d = doublet, t = triplet, q = quintet. The chemical shifts are reported relative to 0.3 M ⁶LiCl/MeOH at -100 °C (0.0 ppm) and [¹⁵N]aniline (52 ppm). All *J* values are reported in hertz. ¹³C–Si resonances are all poorly resolved (see supporting information) and are not listed. Solvent carbon numbering is indicated in Chart 1. ^b Recorded at -120 °C. ^c Not recorded due to difficulties associated with large binding energy differences.

spectroscopy provided important insight into solvation. The appearance of monosolvated dimer **3a** and subsequent replacement by disolvated dimer **1a** in the ⁶Li and ¹⁵N NMR spectra are accompanied by the appearance of two distinct sets of resonances corresponding to the bound THF ligand in the ¹³C NMR spectra (Figure 2, A and B). As the added THF exceeds 1.0 equiv per Li, the ¹³C NMR spectra reveal disolvated dimer **1a** along with resonances corresponding to uncoordinated THF (Figure 2C). Additional THF causes enhanced intensity of the resonances of the free ligand accompanied by no other spectral changes. Thus, dimer **1a** is clearly a disolvate as drawn. In contrast, the monomer **2a** appears at relatively high donor solvent concentrations (mandating less direct methods for determination of solvation numbers discussed in a more appropriate context below). These spectral changes are accompanied by predicted changes in the trimethylsilyl carbon resonances.

In some cases, the NMR spectra reveal asymmetry imparted by the solvent. For example, the monosolvate of *n*-BuOMe shows two distinct trimethylsilyl groups consistent with the depiction **8**. (The alignment of the C–O–C and (NLi)₂ planes is based upon crystallographic analogy.²) Similarly, the chirality of 2-MeTHF is manifested by four trimethylsilyl carbon resonances (**9**). This suggests substantially restricted rotation about the solvent–lithium bond.



The spectral properties of mono- and disolvated dimers of LiHMDS are analogous for a range of ethereal solvents (Tables 1 and 2). The most severely hindered ligands such as (*i*-Pr)₂O, 2,2,5,5-Me₄THF, and *tert*-amyl methyl ether are in rapid

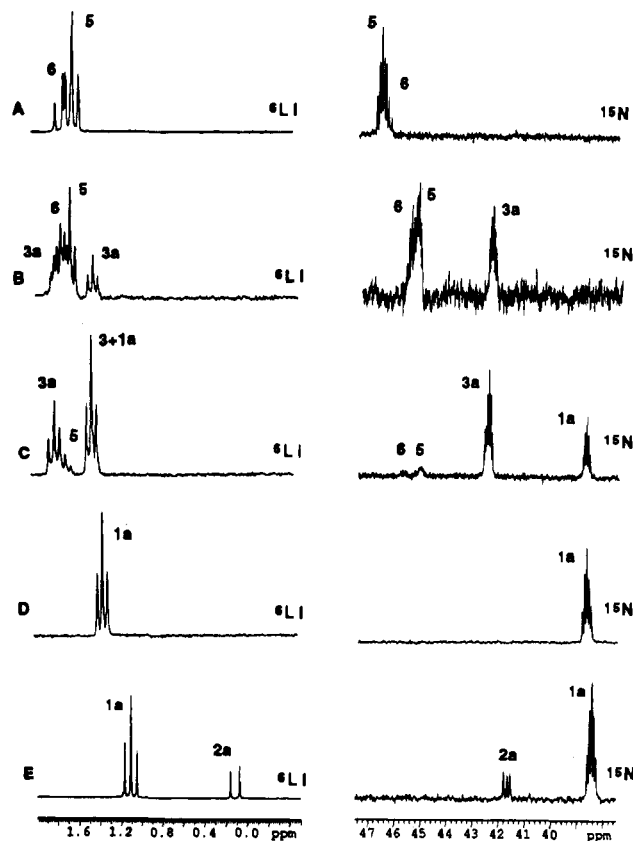


Figure 1. ⁶Li and ¹⁵N NMR spectra of 0.1 M [⁶Li,¹⁵N]LiHMDS in pentane at -100 °C: (A) no added ligand; (B) 0.3 equiv of THF per Li; (C) 0.7 equiv of THF per Li; (D) 5.0 equiv of THF per Li; (E) 40 equiv of THF per Li (33% by volume).

exchange on NMR time scales even at the lowest accessible temperatures (≤ -120 °C in toluene-*d*₈). The monomer–dimer proportions are highly solvent dependent (discussed below).

Chart 2

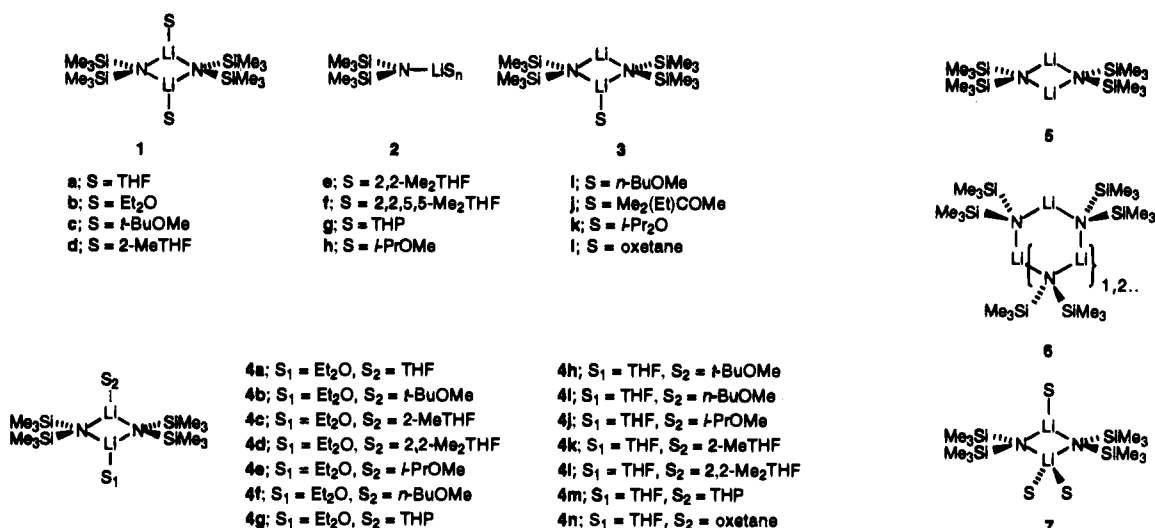


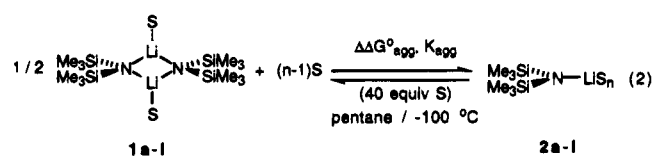
Figure 2. Partial ¹³C NMR spectra of 0.10 M [⁶Li]LiHMDS in toluene-*d*₈ at -100 °C with the following amounts of added ligand (per Li): (A) 0.7 equiv of THF; (B) 1.1 equiv of THF; (C) 2.0 equiv of THF.

Watching LiHMDS in the limit of slow solvent exchange allowed us to observe and study mixed-solvated dimers as well. For example, ⁶Li and ¹⁵N NMR spectra recorded on pentane solutions of LiHMDS containing THF (0.5 equiv per Li) and Et₂O (1.0 equiv per Li) display resonances corresponding to **1a** and **1b** along with two new ⁶Li triplets and one new ¹⁵N quintet characteristic of mixed-solvated-dimer **4a**. The ¹³C NMR spectrum in toluene-*d*₈ shows resonances corresponding to coordinated THF and Et₂O ligands of **4a** that are distinct from those of **1a**, **1b**, **3a**, and **3b**. The spectral data for a number of mixed-solvated dimers (**4a-n**) are listed in Table 2.

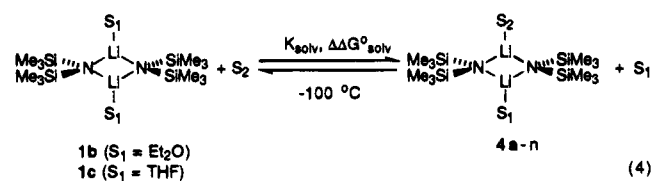
Mechanism of Ligand Substitution. Observation of dimers in the limit of slow solvent exchange afforded information pertaining to ligand substitution that has been elusive to date. The temperatures at which the ¹³C resonances of disolvated dimers and the free ligands coalesce are invariant (±5.0 °C) over 20-fold changes in free solvent concentrations (0.2–5.0 equiv per Li excess). This indicates that the ligand substitution of disolvated dimers (**1**) occurs by a dissociative mechanism via the monosolvated dimers (**3**).²⁸ The approximate correlation of increasing ligand exchange rates with increasing steric demands (Table 3) can be ascribed to destabilization of the sol-

vated dimers relative to the ligand dissociation transition structure (see below). The exception is oxetane; a marked reduction in the coalescence temperature with increasing free oxetane concentration reveals contributions from an associative substitution, presumably via transiently formed trisolvated dimers (**7**).²⁹

Correlation of Aggregation and Solvation Energies. To understand the origins of the odd solvent effects depicted in eq 1 and solvent-dependent aggregation in a more general sense, we sought independent measures of solvation energy and aggregation energy. Solvent-dependent LiHMDS aggregation energies (ΔΔ*G*^o_{agg}, Table 3) in a variety of ethereal solvents (Table 3) were determined by integration of ⁶Li resonances corresponding to the monomers and dimers under standardized conditions (eqs 2 and 3). We evaluated two independent measures of dimer solvation energy. By adjusting the proportions of two competing solvents, integration of the ¹³C resonances corresponding to the unbound donor solvents as well as those coordinated to the symmetrically solvated and mixed solvated dimers (**1a-l** and **4a-n**, respectively) affords relative solvation free energies (ΔΔ*G*^o_{solv}) according to eqs 4 and 5.



$$K_{\text{agg}} = 12 / ([1]^{1/2}[\text{S}]^{n-1}) = \exp(-\Delta\Delta G_{\text{agg}}^\circ / RT) \quad (3)$$



$$K_{\text{solv}} = [4][\text{S}_1] / [1][\text{S}_2] = \exp(-\Delta\Delta G_{\text{solv}}^\circ / RT) \quad (5)$$

The integrations of several solvent-derived ¹³C resonances and independent determinations using THF and Et₂O as the standards provided strong corroboration (Table 3). For each solvent pair, conditions affording the mixed-solvated dimer also afforded coexistence of the two homosolvated dimers in proportions shown to be nearly statistical.²² This demonstrates that the ligands on one lithium of the mixed-solvated dimers do not

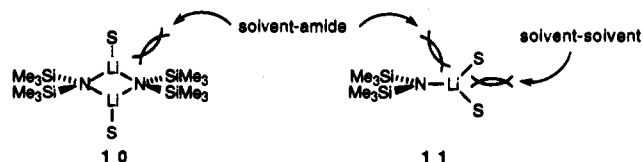
Table 3. Experimentally Derived Thermodynamic Parameters

solvent, S	[2]:[1] ^a	$\Delta\Delta G^\circ_{\text{agg}}^b$	$\Delta\Delta H^\circ_{\text{agg}}^c$	$\Delta\Delta S^\circ_{\text{agg}}^c$	T_{coal}^d	$\Delta\Delta G^\circ_{\text{act}}^d$	$\Delta\Delta G^\circ_{\text{solv}}^e$
Et ₂ O	1:49	2.6	0.00	-4	-76	8.6	2.3
<i>t</i> -BuOMe	1:2.8	1.6	0.08	-9	-105	7.4	3.5 ^h
THF	1:2.6	1.6	-0.42 ^f	-11 ^f	-47	10.8	0.0
2-MeTHF	1:7.3	1.9	0.79	-6.7	-56	10.0	0.6
2,2-Me ₂ THF	34:1	0.6	-0.10	-4.8	-85	8.9	1.7
<i>n</i> -BuOMe	1:99	2.8	<i>g</i>	<i>g</i>	-53	9.8	1.2
<i>i</i> -PrOMe	1:27	2.3	-0.10	-13	-72	8.9	2.0 ^h
THP	1:19	2.2	0.00	-13	-50	10.6	0.3
Me ₂ (Et)COMe	1:7.2	1.9	0.02	-11	<i>i</i>	<i>i</i>	<i>i</i>
oxetane ^j	1:12	0.5	-1.9	-14	<i>i</i>	<i>i</i>	-0.3 ^k
oxetane ^l	42:1	0.1	-3.5 ^f	-20 ^f	<i>i</i>	<i>i</i>	<i>i</i>

^a Relative proportions of monomer (2) and dimer (1) determined from ⁶Li integrations of 0.1 M LiHMDS in pentane with 4.0 M donor solvent at -100 °C. ^b Aggregation free energies as determined from the monomer:dimer ratio according to eqs 2 and 3 (± 0.2 kcal/mol per Li). ^c Enthalpy of aggregation ($\Delta\Delta H^\circ_{\text{agg}}$, ± 0.3 kcal/mol per Li) and entropy of aggregation ($\Delta\Delta S^\circ_{\text{agg}}$, ± 2 cal/(mol·deg) per Li) determined from the temperature dependence (-20 to -100 °C) of the monomer:dimer ratio (eq 1). ^d Temperature dependencies were determined at 40 equiv of donor solvent with the following exceptions: Et₂O (80 equiv), 2,2-Me₂THF (30 equiv), and oxetane (5 and 20 equiv). ^e T_{coal} (± 3 °C) corresponds to the temperature at which the α carbons of the coordinated and free solvent resonances coalesce; $\Delta\Delta G^\circ_{\text{act}}$ (± 0.3 kcal/mol) corresponds to the affiliated activation barrier. ^f $\Delta\Delta G^\circ_{\text{solv}}$ (± 0.2 kcal/mol) corresponds to the average of the values determined relative to Et₂O and THF according to eqs 4 and 5. ^g Value distorted by curvature (Figure 6). ^h Quantitative measurement was precluded by low LiHMDS monomer concentration; however, there appeared to be no temperature dependence indicating a near-zero $\Delta\Delta H^\circ_{\text{agg}} \approx 0$ kcal/mol. ⁱ $\Delta\Delta G^\circ_{\text{solv}}$ determined relative to Et₂O according to eqs 4 and 5. ^j Solvent exchange is rapid on NMR time scale. ^k 5.0 equiv of oxetane per Li. ^l Crudely estimated by displacement of THF observed in ⁶Li and ¹³C NMR spectra. ^m 20 equiv of oxetane per Li.

influence the energy of solvation on the second site. The relative solvation energies were determined under conditions where the mixed-solvated and one homosolvated dimer dominated. Alternatively, since the mechanism for ligand substitution was shown to be dissociative via rate-limiting cleavage of the solvent–lithium bond, the measured activation energies ($\Delta\Delta G^\circ_{\text{act}}$) should reflect the absolute solvation energies. Despite the fact that the various $\Delta\Delta G^\circ_{\text{act}}$ are not isothermal, a plot of $\Delta\Delta G^\circ_{\text{act}}$ vs $\Delta\Delta G^\circ_{\text{solv}}$ shows a very strong 1:1 correlation (Figure 3). We suspect that the strong correlation stems from a very late transition state and that the values of $\Delta\Delta G^\circ_{\text{act}}$ approximate absolute free energies of dimer solvation.

The independent measures of aggregation energy ($\Delta\Delta G^\circ_{\text{agg}}$) and dimer solvation energy ($\Delta\Delta G^\circ_{\text{solv}}$) allowed us to ask a question of central importance: Does the observable LiHMDS aggregation state correlate with the strength of the solvent–lithium interaction? In short, the answer is no. A plot of $\Delta\Delta G^\circ_{\text{agg}}$ vs $\Delta\Delta G^\circ_{\text{solv}}$ (Figure 4) shows no discernible correlation. We surmised that the solvent–amide interactions in the dimer are more severe than those found in the monomer (cf. 10 and 11). Promotion of the monomer by moderately hindered



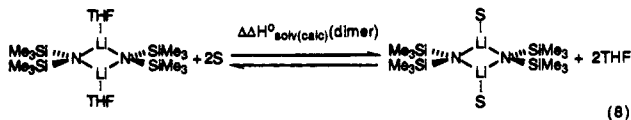
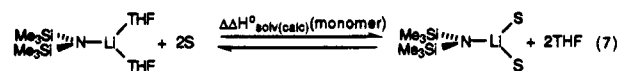
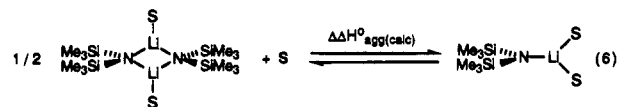
donor solvents (e.g. 2,2-Me₂THF) might be a consequence of the relatively uncongested monomer coordination sphere. The solvent–solvent interactions within the monomer (see 11) could become dominant for extremely hindered donor solvents (e.g. 2,2,5,5-Me₄THF). The resulting relative stabilization of the

(28) Under conditions where the two resonances in undergoing coalescence are in 1:1 proportions, the relationship of the rate constant and coalescence temperature can be approximated as $\Delta G_{\text{act}} = -RT \ln(k_{\text{obs}}/kT_{\text{coalesc}})$ such that $k_{\text{obs}} = 2.22\Delta\nu$. If we assume that k_{obs} is proportional to the concentration of free donor solvent, then we find that the coalescence temperature (T_{coalesc}) for an associative substitution would change by approximately 20 °C over the free donor solvent concentration range studied.

(29) Depue, J. S.; Collum, D. B. *J. Am. Chem. Soc.* **1988**, *110*, 5518. Seebach, D.; Bauer, W.; Hansen, J.; Laube, T.; Schweizer, W. B.; Dunitz, J. D. *J. Chem. Soc., Chem. Commun.* **1984**, 853. Williard, P. G.; Liu, Q.-Y. Unpublished. See also ref 30.

dimer (or, more appropriately, relative destabilization of the monomer) would cause the solvated dimer to predominate. (The loss of higher unsolvated oligomer and the chemical shift of the resulting dimer demonstrates the dimer in 2,2,5,5-Me₄THF to be solvate **1f** rather than unsolvated dimer **5**.) The conclusion is clear: the measured relative dimer solvation energies are inadequate as measures of relative solvation energies in general.

The failed correlation of dimer solvation energy and aggregation energy suggests that the dimer and monomer solvation energies are not strongly correlated. We explored this point further using semiempirical (MNDO) computational methods (eqs 6–8). We will show that the model based upon disolvated



monomers, while founded on seemingly sound indirect evidence (see Discussion), is *not* correct. However, at the time this was not fully appreciated, and more to the point, MNDO is too sterically sensitive to evaluate the stabilities of trisolvated monomers.^{30,31} With this in mind, we present the studies as follows. Although the sensitivity of MNDO to steric effects would be expected to preclude a quantitative theory–experiment correlation, a plot of the experimentally observed $\Delta\Delta G^\circ_{\text{agg}}$ vs $\Delta\Delta H^\circ_{\text{agg}}(\text{calc})$ (eq 6; see supporting information) does not afford even a qualitative correlation. Contrary to our supposition noted above, we observe a strong correlation of the calculated monomer solvation enthalpies (eq 7) and dimer solvation enthalpies (eq 8). We considered three possible explanations for the failed theory–experiment correlation: (1) MNDO is hopelessly flawed or at least too imprecise. While this is certainly plausible, qualitative theory–experiment correlations for lithium dialkylamide equilibria have been remarkably successful.^{11,30,31} (2) The model based upon disolvated mono-

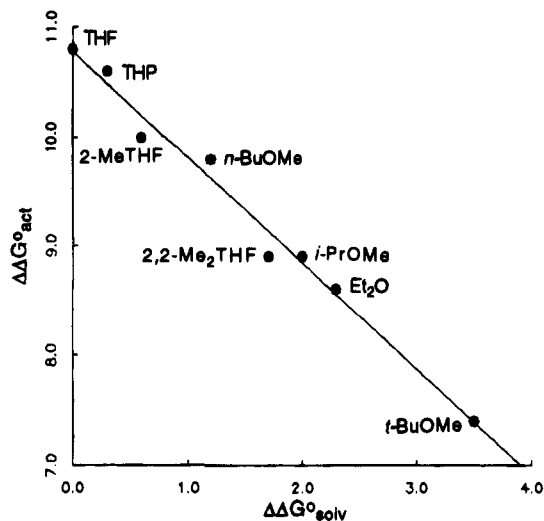


Figure 3. Plot of activation free energies for dissociative ligand exchange on LiHMDS dimer 1 ($\Delta\Delta G^\circ_{\text{act}}$, Table 3) vs LiHMDS dimer solvation energies ($\Delta\Delta G^\circ_{\text{solv}}$) as described by eqs 2–5 and listed in Table 3.

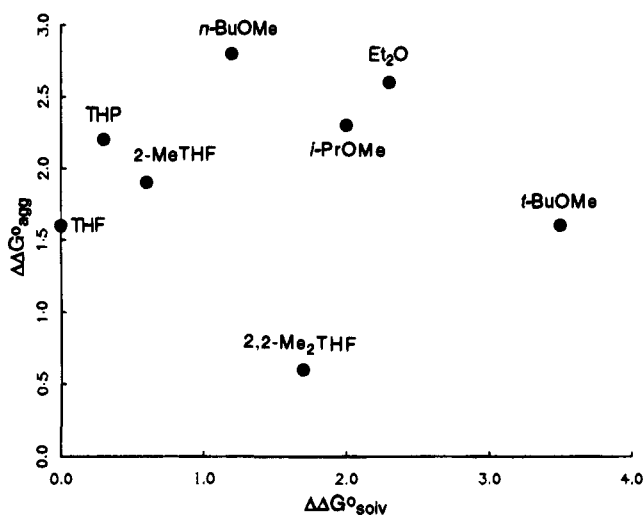


Figure 4. Plot of LiHMDS aggregation free energies ($\Delta\Delta G^\circ_{\text{agg}}$, Table 3) vs LiHMDS dimer solvation energies ($\Delta\Delta G^\circ_{\text{solv}}$, eqs 4 and 5, Table 3).

mers, while supported by seemingly sound indirect evidence (discussed below), is not correct. (3) The calculated *enthalpies* are poor approximations of measured *free energies* in this particular context.

Point (3) was addressed by determining the experimental aggregation enthalpies ($\Delta\Delta H^\circ_{\text{agg}}$). Monitoring the monomer–dimer proportions under the conditions prescribed in eq 2 (yet over an 80 °C temperature range) revealed nearly temperature-independent equilibria ($\Delta\Delta H^\circ_{\text{agg}} \approx 0$) for the majority of ethereal solvents (Table 3). This is a remarkable result in a field characterized by highly temperature-dependent equilibria. The independence of $\Delta\Delta H^\circ_{\text{agg}}$ on donor solvent indicates that the solvent dependence of the LiHMDS monomer–dimer equilibrium must be ascribed to variations in the internal entropy. (We hasten to add that the numerical representations of $\Delta\Delta S^\circ_{\text{agg}}$

(30) Romesberg, F. E.; Collum, D. B. *J. Am. Chem. Soc.* **1992**, *114*, 2112.

(31) Romesberg, F. E.; Collum, D. B. *J. Am. Chem. Soc.* **1994**, *116*, 9187. Bernstein, M. P.; Romesberg, F. E.; Fuller, D. J.; Harrison, A. T.; Collum, D. B.; Liu, Q.-Y.; Williard, P. G. *J. Am. Chem. Soc.* **1992**, *114*, 5100.

(32) Manifestation of a steric effect as an entropic contribution has been referred to as “population control”. Winans, R. E.; Wilcox, C. F., Jr. *J. Am. Chem. Soc.* **1976**, *98*, 4281.

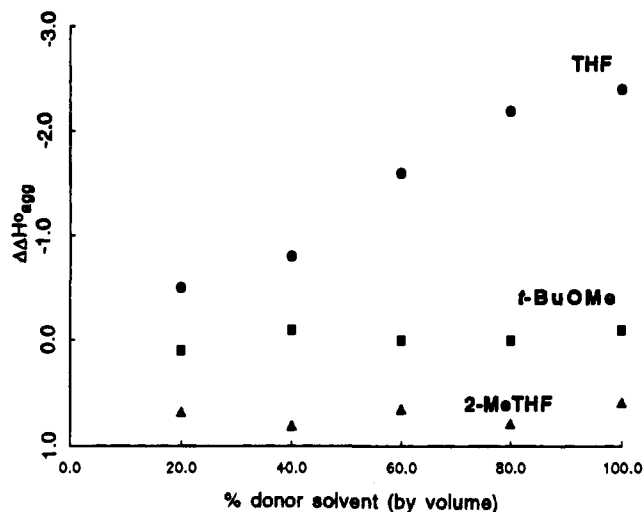


Figure 5. Measured aggregation enthalpies ($\Delta\Delta H^\circ_{\text{agg}}$, Table 4) vs donor solvent concentrations (in pentane) determined over the temperature range from -20 to -100 °C.

in Table 3 are a consequence of pragmatism and should be interpreted, at best, qualitatively out of respect for the enormous errors associated with most entropy determinations.³²

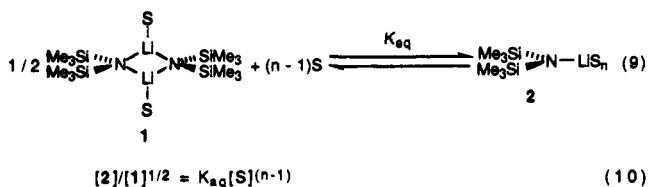
The temperature independence of the monomer–dimer equilibrium in the presence of 40 equiv of THF (33% by volume) was particularly striking in light of Kimura and Brown’s studies showing a substantial temperature dependence in *neat* THF.²⁰ If the LiHMDS monomer and dimer solvation numbers remain constant over the range of solvent concentrations, the measured aggregation enthalpy should be independent of donor solvent concentration. For example, $\Delta\Delta H^\circ_{\text{agg}}$ for LiHMDS in 2-MeTHF/pentane and *t*-BuOMe/pentane mixtures shows no discernible dependence on the donor solvent concentrations (Table 3 and Figure 5). In contrast, $\Delta\Delta H^\circ_{\text{agg}}$ in THF/pentane mixtures displays a marked enthalpic stabilization of the monomer with increasing THF concentration (Figure 5). In neat THF, we observe strongly temperature-dependent monomer–dimer proportions with the measured aggregation enthalpy ($\Delta\Delta H^\circ_{\text{agg}} = 2.4 \pm 0.3$ kcal/mol). The van’t Hoff plot (Figure 6) displays a curvature consistent with such a temperature-dependent shift in solvation number. The slight disagreement with the value of 2.0 kcal/mol reported by Kimura and Brown stems from the curvature in conjunction with our expanded temperature range.

We submit that the enthalpic preference for LiHMDS monomer at elevated THF concentrations stemmed from a [THF]-dependent solvation state change. That is not to say, however, that the drifting enthalpy can necessarily be ascribed to the appearance of an enthalpically more stable monomer higher solvate. In principle, the dimer could be undergoing a shift to an enthalpically disfavored, yet mass action favored, higher solvate. Evidence delineated below supports shifting monomer solvation.

Monomer Solvation Numbers. We turned to a conceptually simple strategy for determining LiHMDS monomer solvation numbers.^{33,34} The monomer–dimer equilibrium (eq 9) should manifest a solvent dependence described by eq 10. We leave unjustified for the moment the assumed static disolvated dimer structure and note that the experiment determines only the

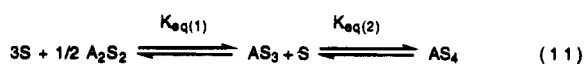
(33) Evidence of a trisolated lithiated imine monomer: Kallman, N.; Collum, D. B. *J. Am. Chem. Soc.* **1987**, *109*, 7466.

(34) (a) Waack, R.; Doran, M. A.; Stevenson, P. E. *J. Am. Chem. Soc.* **1966**, *88*, 2109. (b) Chan, L. L.; Smid, J. *J. Am. Chem. Soc.* **1967**, *89*, 4547. (c) Chan, L. L.; Wong, K. H.; Smid, J. *J. Am. Chem. Soc.* **1970**, *92*, 1955.



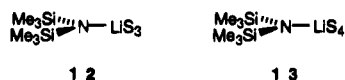
relative monomer and dimer solvation numbers. Several ethereal solvents offer measurable monomer and dimer concentrations over a substantial solvent concentration range. Figure 7 shows a plot of $[\text{monomer}]/[\text{dimer}]^{1/2}$ vs $[t\text{-BuOMe}]$ at both -20 and -80 °C; the complete superposition of the two data sets is a consequence of the temperature independence of the ratios. The function in Figure 7 would be linear if the monomers are disolvated ($n = 2$); the upward curvature clearly argues against exclusive formation of disolvated monomers. Non-linear least-squares fit to eq 10 affords $n = 3.1 \pm 0.1$ at both temperatures (Table 4) consistent with exclusive formation of trisolvated monomer. Similarly, studies of LiHMDS in 2-MeTHF/pentane mixtures afford [2-MeTHF]-independent $\Delta\Delta H^\circ_{\text{agg}}$ and temperature-independent solvation numbers consistent with formation of trisolvated monomer (Table 4).

Quite different results are obtained for LiHMDS in THF-pentane. The LiHMDS monomer-dimer proportions measured in a range of THF concentrations at -20 °C (Table 4, Figure 8) are consistent with nearly exclusive formation of trisolvated monomer (12). As the temperature is decreased the measured



$$[\text{AS}_n]_{\text{total}}/[\text{A}_2\text{S}_2]^{1/2} = K_{\text{eq}(1)}[\text{S}]^2(K_{\text{eq}(2)}[\text{S}] + 1) \quad (12)$$

relative solvation numbers increase, approaching values of “ n ” consistent with appearance of a *tetrasolvated* monomer (13). The retention of strong N-Li coupling ($J_{\text{Li-N}} = 5.0$ Hz) over all conditions indicates that the monomer retains a distinct N-Li contact. Although the simple polynomial expression in eq 10 adequately uncovered the evidence of intervening tetrasolvated monomer, the overall scenario can now be more accurately described by eqs 11 and 12 where $[\text{AS}_n]_{\text{total}}$ is the total monomer concentration and A_2S_2 , AS_3 , and AS_4 correspond to 1, 12, and 13 (respectively). (The derivation of eq 12 is included as



supporting information.) Nonlinear least-squares fit to eq 12 affords an excellent fit to the data. While the fit to eq 12 does not offer a statistically significant improvement over the fit to the simple polynomial expression in eq 10, the adjustable parameters $K_{\text{eq}(1)}$ and $K_{\text{eq}(2)}$ afford predicted ratios of the three species as a function of THF concentration (Figure 9).

The temperature-dependent solvation numbers and [THF]-dependent enthalpies afford a self-consistent picture; however, the implication of a *tetrasolvated* contact-ion-paired monomer is, at best, strongly contrary to conventional notions of lithium coordination chemistry. We posited that the superior ligating properties of oxetane³⁵ might promote tetrasolvate formation even better than THF. In accord, we found the following: (1) The LiHMDS monomer appears at unusually low oxetane concentrations (≥ 5.0 equiv per Li), and its concentration increases sharply with increasing oxetane concentration (when

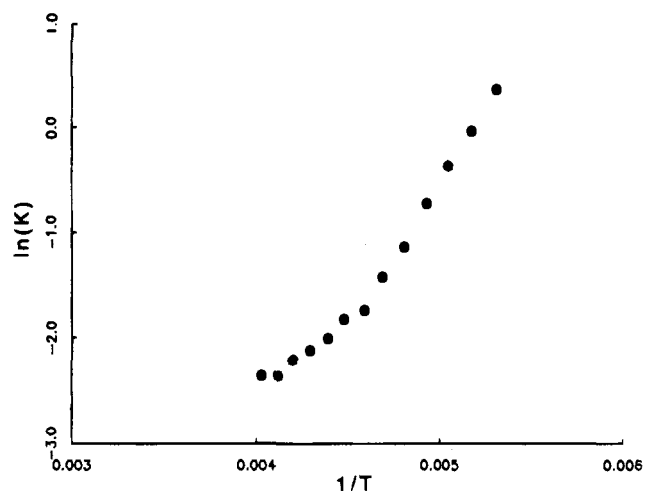


Figure 6. Temperature dependence of the monomer-dimer proportions (eq 1) for 0.1 M LiHMDS in pentane containing 75 equiv of THF per Li.

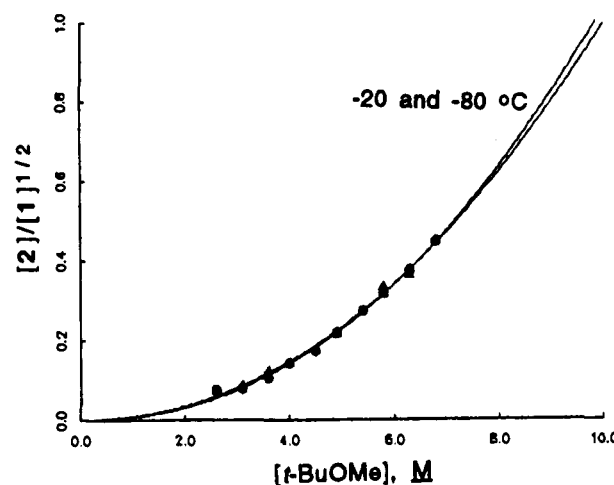


Figure 7. Plot of $[2]/[1]^{1/2}$ vs $[t\text{-BuOMe}]$ for 0.1 M LiHMDS in pentane at -20 and -80 °C. The data are fit by non-linear least-squares methods to the function in eq 10 (-20 °C, $K_{\text{eq}} = 7.9 \pm 0.5 \times 10^{-3}$, $n = 3.1 \pm 0.1$; -80 °C, $K_{\text{eq}} = 7.4 \pm 0.4 \times 10^{-3}$, $n = 3.1 \pm 0.1$).

Table 4. Solvation Number (n) of LiHMDS Monomer 2 Determined According to Eqs 9 and 10^a

	-20 °C	-80 °C
THF	3.0 ± 0.1	3.6 ± 0.2
<i>t</i> -BuOMe	3.1 ± 0.1	3.1 ± 0.1
2-MeTHF	2.9 ± 0.2	3.1 ± 0.1
oxetane	3.7 ± 0.2	<i>b</i>
2,2-Me ₂ THF	<i>c</i>	3.1 ± 0.2

^a Solvation numbers were determined from ⁶Li NMR spectra recorded on 0.1 M solutions of [⁶Li]LiHMDS in pentane with varying concentrations (> 1.0 M) of added donor solvent. Error bars correspond to one standard deviation. ^b Determination precluded by inordinately high rate of appearance of monomer at low oxetane concentrations. ^c Determination precluded by coalescence of resonances.

compared to THF). (2) The temperature dependence of the LiHMDS monomer-dimer ratio at different oxetane concentrations reveals drifting aggregation enthalpies akin to that observed for THF shown in Figure 5. (3) Measured oxetane solvation numbers (eqs 9 and 10, Table 4) show a drift toward tetrasolvated LiHMDS monomer with increasing oxetane concentration and decreasing temperature that is more pronounced than seen with THF. (4) At oxetane concentrations suggested to afford a mixture of tri- and tetrasolvated LiHMDS monomer, the ⁶Li and ¹⁵N NMR spectra reveal *two spectroscopically distinct monomers* (Figure 10). The high activation free energy for

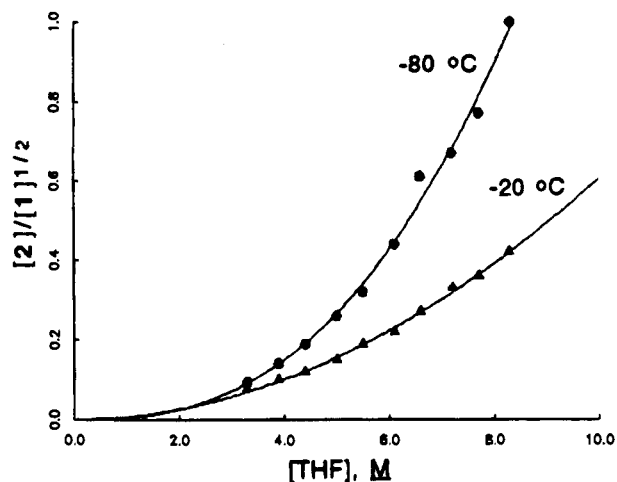


Figure 8. Plot of $[2]/[1]^{1/2}$ vs $[THF]$ for 0.1 M LiHMDS in pentane at -20 and -80 °C. The data are fit by nonlinear least-squares methods to the function in eq 10 (-20 °C, $K_{eq} = 6.8 \pm 0.6 \times 10^{-3}$, $n = 3.0 \pm 0.1$; -80 °C, $K_{eq} = 4.2 \pm 0.8 \times 10^{-3}$, $n = 3.6 \pm 0.2$).

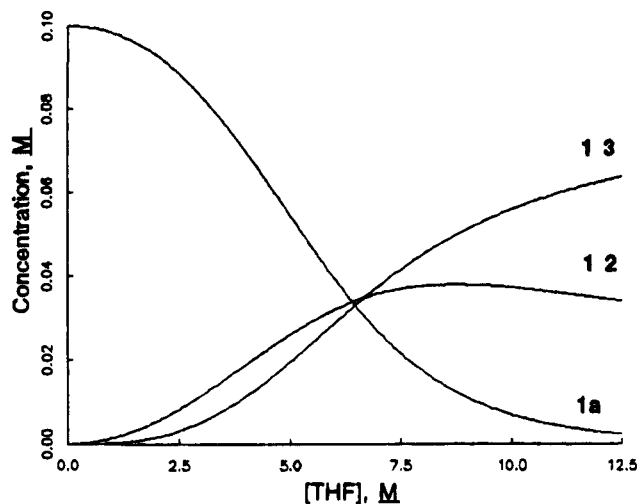


Figure 9. Predicted concentrations of disolvated dimer **1a**, trisolvated monomer **12** ($S = THF$), and tetrasolvated monomer **13** ($S = THF$). The functions are calculated using adjustable parameters $K_{eq(1)} = 4.0 \times 10^{-5}$ and $K_{eq(2)} = 1.5 \times 10^{-1}$ derived from nonlinear least-squares fit to eq 12. (See supporting information for derivations.)

exchange of 9.7 ± 0.3 kcal/mol ($T_{coalescence} = -90$ °C) is consistent with the evidence pointing to considerable enthalpic stabilization of the putative tetrasolvate. The oxetane concentration predicted from the numerical fits to afford equimolar tri- and tetrasolvated monomer coincides quite well with the oxetane concentration affording equimolar concentrations of the two spectroscopically distinct monomers. We defer further discussion of primary vs secondary shell solvation effects to the discussion section.

Discussion

To the best our knowledge lithium hexamethyldisilazide is the only lithium salt for which monodentate ethereal solvent exchange is slow on NMR time scales.³⁶ (See Note Added in Proof). As a consequence, we were afforded a unique opportunity to address a number of fundamental questions and issues that have remained elusive for many years. We observed

(36) Spectroscopic evidence of ether coordination in the slow exchange limit has recently been attributed to conformational effects instead: Boche, G.; Fraenkel, G.; Cabral, J.; Harms, K.; van Eikema Hommes, N. J. R.; Lohrenz, J.; Marsch, M.; Schleyer, P. v. R. *J. Am. Chem. Soc.* **1992** *114*, 1562.

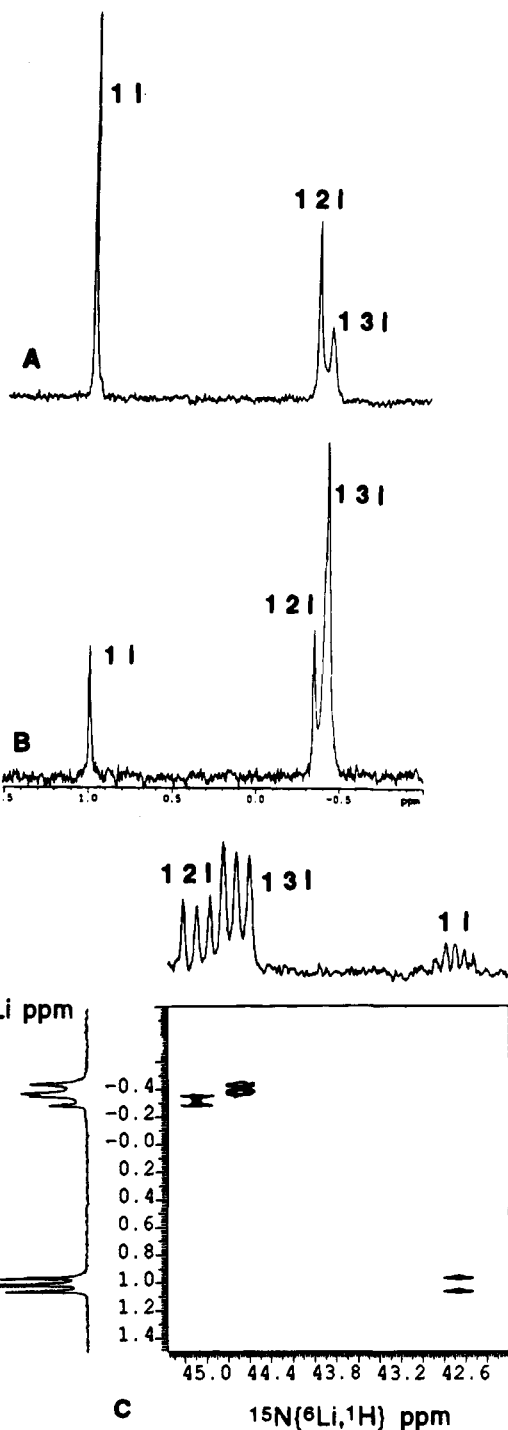


Figure 10. 6Li NMR spectra of 0.1 M $[{}^6Li]$ LiHMDS in pentane at -110 °C containing (A) 10 equiv of oxetane per Li and (B) 17 equiv of oxetane per Li. Spectrum (C) is a 6Li - ${}^{15}N$ HMQC spectrum of 0.10 M $[{}^6Li, {}^{15}N]$ LiHMDS in pentane containing with 13 equiv of oxetane per Li.

and fully characterized mono-, di-, and mixed-solvated dimers (**3**, **1**, and **4**, respectively) for a considerable variety of ethereal solvents. Careful ${}^{13}C$ resonance integration confirmed previous suspicions^{11,24,30,31} that the LiHMDS dimers are disolvated rather than tri- or tetrasolvated at low (1.0–10 equiv/Li) donor solvent concentration. Solvent exchange on the dimer proceeds via rate-limiting dissociation to give monosolvated dimers (**3**) rather than via an associative mechanism via trisolvated dimers (**7**). Until now, the simple yet fundamental distinction of associative vs dissociative ethereal ligand substitution at lithium ions had not been achieved. In principle, decreased steric demands of the solvent and R_2N fragment should enhance the probability of

observing slow solvent exchange. However, in the case of oxetane, concentration-dependent exchange rates reveal that an associative substitution via trisolvated dimers (7) can be competitive with the dissociative substitution pathway. In fact, the associative substitution mechanism may dominate for most ethers at high ether concentrations. LiHMDS provides a delicate balance between associative and dissociative ligand substitutions—a balance that renders it optimal for observing slow solvent exchange. Other organolithium-solvent combinations that constitute marked increases or decreases in the overall steric congestion might experience rapid ether ligand exchange.

The slow solvent exchange afforded a direct determination of relative free energies of dimer solvation ($\Delta\Delta G^{\circ}_{\text{solv}}$) for a range of ethereal solvents. Unlike calorimetrically determined enthalpies,⁵ these solvation free energies are not complicated by structural ambiguities. There were no real surprises. THF was found to bind more strongly than Et₂O by 2.3 kcal/mol per lithium. Increased solvent steric demands generally afford more positive $\Delta\Delta G^{\circ}_{\text{solv}}$. During the course of these studies we also obtained insight into the energetics of mixed solvation. Mixed-solvated dimers (4) show no cooperativity of binding at the two lithium sites; the presence and structure of the ethereal solvent on one lithium has little influence on the propensity of the second lithium site to undergo solvation. The common practice of using solvent combinations as well as the strong evidence implicating substrate precomplexation³⁷ (presumably in cooperation with coordinated donor solvents) highlights the importance of understanding the principles underlying mixed solvation.³⁸

At elevated donor solvent concentrations we observe monomers whose concentrations vary sensitively and unpredictably as a function of donor solvent structure (see eq 1 and Table 3). Contrary to conventional wisdom, the free energies of aggregation ($\Delta\Delta G^{\circ}_{\text{agg}}$; eq 3) and the free energies of dimer solvation ($\Delta\Delta G^{\circ}_{\text{solv}}$; eq 5) do not correlate whatsoever (Figure 4). This underscores a very important point: *Superior donor solvents do not necessarily promote deaggregation.* We originally couched our explanation for these odd trends in terms of competing solvent–amide and solvent–solvent interactions depicted by 10 and 11. A dimer preference with unhindered solvents such as Et₂O seemed logical to the extent that the stabilization derived from aggregation would be minimally offset by destabilizing solvent–amide interactions in the congested dimer coordination sphere. The tendency of moderately bulky solvents such as *t*-BuOMe to promote monomer formation could be ascribed to steric relief of enhanced solvent–amide interactions in the dimer. This odd relationship of solvation energy and observed aggregation energy had been foreshadowed by several previous investigations.^{16,24} However, we completely failed to anticipate that the sterically most demanding donor solvents such as 2,2,5,5-Me₄THF would cause a selectivity reversal, with the disolvated dimer becoming the most stable (least destabilized) form. We ascribed this reversal to solvent–solvent interactions in the monomer becoming dominant only in the limit of high solvent steric demand. This complex, yet relatively satisfying, model for solvent-dependent aggregation came into question when an MNDO computational study of the monomer–dimer equilibrium provided an unsatisfactory correlation of calculated aggregation enthalpies ($\Delta\Delta H^{\circ}_{\text{agg}(\text{calc})}$) and observed $\Delta\Delta G^{\circ}_{\text{agg}}$. Further experimental scrutiny revealed the model to be fundamentally flawed in two important ways.

First, noting that the experiments provided the solvent-dependent free energies of aggregation while MNDO affords enthalpies, we measured the temperature dependencies of the

monomer:dimer ratios to determine the experimental values of $\Delta\Delta H^{\circ}_{\text{agg}}$. Of the nine ethereal solvents showing sufficient concentrations of both monomer and dimer to allow determination of an observable aggregation energy, seven displayed temperature-independent monomer:dimer ratios ($\Delta\Delta H^{\circ}_{\text{agg}} \approx 0$ kcal/mol). It is not surprising that an observable monomer–dimer mixture manifests a near-zero $\Delta\Delta H^{\circ}_{\text{agg}}$ since displacement substantially from zero could prevent appreciable coexistence of both forms. The solvents for which $\Delta\Delta H^{\circ}_{\text{agg}}$ could not be measured due to an inadequate coexistence of monomer and dimer (*i*-Pr₂O and 2,2,5,5-Me₄THF) may or may not have substantially non-zero $\Delta\Delta H^{\circ}_{\text{agg}}$. Nevertheless, the fact that seven different ethereal solvents affording monomer:dimer ratios spanning a 250-fold range display invariant enthalpies seems extraordinary. We conclude that the substantial solvent dependence on the monomer–dimer proportions must stem from solvent-dependent entropies of aggregation ($\Delta\Delta S^{\circ}_{\text{agg}}$). We hasten to add that the translational entropy component associated with a change in particle number upon solvent-assisted deaggregation will be solvent-independent (assuming solvent independent solvation numbers; see below). Consequently, the solvent dependence must be on the molar entropies associated with ordering the solvents within the monomer and dimer lithium coordination spheres.²³ In essence, the organization of solvents within the lithium coordination sphere so as to minimize the enthalpic problems will differ for the monomer and dimer. It is this difference that depends on the precise structural details of the solvent. A clear understanding of the solvent-dependent $\Delta\Delta S^{\circ}_{\text{agg}}$ will require considerable further investigation.

A second flaw in our explanation for the solvent-dependent aggregation was revealed by studies of monomer solvation number. Mounting indirect evidence led us to postulate that the monomers of LiHMDS (and other hindered lithium dialkylamides) exist as disolvates 11.^{10,11,30,31} Although semiempirical calculations appear to be hypersensitive to extreme steric effects, the failure of MNDO to afford minima for trisolvated monomers suggested an inherent instability.^{11,30,31} Similarly, spectroscopic studies of LiHMDS–HMPA solvates as well as other lithium amide–HMPA solvates provide experimental evidence of disolvated monomers.^{10,11,39} Although the computational studies underscored the substantial steric demands of coordinated HMPA, we surmised that simple ethereal solvents would not cause the LiHMDS monomer to exceed the disolvation state. In studies of related lithium anilides, Jackman and co-workers also suggested the monomers to be either disolvated or trisolvated depending upon the steric demands of the anilide and the choice of solvent.⁴⁰ In the event, monitoring the monomer:dimer ratios as a function of ether ligand concentration with the aid of nonlinear least-squares analyses demonstrated that the relatively hindered *t*-BuOMe affords trisolvated LiHMDS monomers.³³ *Even more strikingly, we accrued considerable circumstantial evidence that THF affords appreciable concentrations of tetrasolvated monomer 13.* The evidence of a five-coordinate, tetrasolvated LiHMDS monomer is extensive, self-consistent, and, in our opinion, compelling. It is summarized as follows:

(1) The monomer–dimer equilibrium in 33% THF/pentane shows a temperature independence ($\Delta\Delta H^{\circ}_{\text{agg}} \approx 0$ kcal/mol) akin

(38) Representative examples of crystallographically determined mixed solvation: Zarges, W.; Marsch, M.; Harms, K.; Boche, G. *Chem. Ber.* **1989**, *122*, 2303. Karsch, H. H.; Appelt, A.; Mueller, G. *Organometallics* **1985**, *4*, 1624. Boche, G.; Marsch, M.; Müller, A.; Harms, K. *Angew. Chem., Int. Ed., Engl.* **1993**, *32*, 1032.

(39) Sakuma, K.; Gilchrist, J. H.; Romesberg, F. E.; Cajthaml, C. E.; Collum, D. B. *Tetrahedron Lett.* **1993**, *34*, 5213.

(40) Jackman, L. M.; Scarmoutzos, L. M.; DeBrosse, C. W. *J. Am. Chem. Soc.* **1987**, *109*, 5355.

(37) Klumpp, G. W. *Recl. Trav. Chim. Pays-Bas* **1986**, *105*, 1.

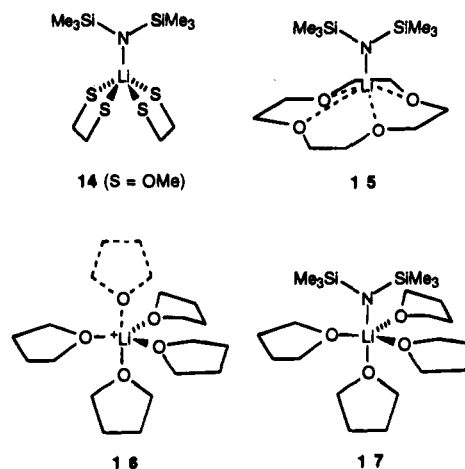
to a substantial number of other ethereal solvents. However, Kimura and Brown noted a sharp temperature dependence with a substantial affiliated aggregation enthalpy favoring monomer ($\Delta\Delta H^\circ_{\text{agg}} \approx 2.0$ kcal/mol (per Li)).²⁰ We confirmed their result by showing that the measured aggregation enthalpy is highly dependent upon the THF concentration as well as uncovered an apparent curvature in the van't Hoff plots consistent with a complex equilibrium. (*t*-BuOMe shows no such effects.) To the extent that $\Delta\Delta H^\circ_{\text{agg}}$ would normally be independent of donor solvent concentration, we inferred that the $\Delta\Delta H^\circ_{\text{agg}}$ was revealing an otherwise undetectable shift in the solvation number. The plausible scenarios included (i) a shift of the monomer to an enthalpically favored higher solvate at high THF concentration or (ii) a shift of the dimer to an enthalpically disfavored (yet mass-action favored) higher solvate.

(2) Although the [THF]-concentration dependencies implicate exclusively trisolvated monomer **12** near ambient temperatures, the measured solvation number increases with decreasing temperature, approaching values suggestive of considerable concentrations of tetrasolvate **13**. The temperature-dependent monomer solvation number is fully consistent with the enthalpic preference for the monomer at elevated THF concentrations described in part (1). Once again, *t*-BuOMe shows clear evidence of only trisolvated monomer **12** at all temperatures.

(3) It was not at all clear that the evidence described in parts (1) and (2) could be uniquely ascribed to a "tetrasolvated monomer" with five-coordinate lithium bearing $(\text{Me}_3\text{Si})_2\text{N}^-$ and four THFs as discrete ligands. The presence of a coordinated amide fragment is confirmed by typical $^6\text{Li}-^{15}\text{N}$ coupling. However, one could imagine a plausible scenario wherein a trisolvated monomer is stabilized by an ill-defined "medium effect"—a sterically insensitive secondary solvation shell. We presumed that oxetane would be better than THF as a ligand for the LiHMDS monomer. In accord, we find that (i) oxetane affords monomer at very low oxetane concentrations (lower than for THF), (ii) the enthalpy of aggregation shows a strong oxetane-concentration dependence, and (iii) measured oxetane solvation numbers increase with decreasing temperature to afford values consistent with the appearance of considerable concentrations of tetrasolvated monomer at low temperatures. While the apparent role of oxetane as a "super" THF equivalent does not, in itself, distinguish primary from secondary shell solvation, during the course of these studies we observed and characterized two distinct monomer forms that differ only in the number of coordinated oxetane ligands. Their concentrations correlate quite well with the concentrations of the tri- and tetrasolvate (**12** and **13**, respectively) predicted from the solvation number determinations.

(4) In the event that evidence of tetrasolvate **13** was an artifact stemming from ill-defined medium effects, such evidence should appear for 2-MeTHF as well. (The 2-methyl substituent should have little effect on the bulk properties relative to THF.⁴¹) If, on the other hand, the putative tetrasolvate is a legitimate 5-coordinate lithium complex, the methyl group of 2-MeTHF should be sufficiently bulky to completely preclude its formation. The experimental results revealed exclusively tris(2-MeTHF)-solvated monomer at all temperatures as well as [2-MeTHF]-independent aggregation enthalpies suggesting an absence of a drifting solvation state.

(5) Ongoing studies of chelating ligands reveal an unusual stabilization of the LiHMDS monomer bearing dimethoxyethane (DME) ligands.⁴² The existence of two or more coordinated DME ligands and the importance of the chelation are both demonstrable. We suspect the existence of doubly chelated monomer **14**.



Overall, we find that the experimental data afford fully self-consistent support for the formation of tetrasolvated monomer **13** at low temperatures and high THF concentrations. Nevertheless, does this seem plausible based on conventional models of lithium ion solvation and coordination chemistry? High lithium ion solvation numbers in solution have been implicated by a variety of techniques including measurement of conductivities, transference numbers, and ion mobilities as well as more direct methods based on EXAFS and diffraction methods.⁴³ An example of particular familiarity to us came from a kinetic study of lithium diphenylamide alkylation in which the rates showed a seventh-order dependence on the THF concentration.⁴⁴ However, many of the methods do not distinguish primary-shell solvation from secondary-shell (and higher) solvation. X-ray crystal structures of lithium cryptands and crown complexes and assorted other chelated complexes offer compelling documentation for high-coordinate lithium.⁴⁵⁻⁴⁸ The LiHMDS(12-crown-4) complex (**15**) described by Power and Xiaojie seems particularly pertinent.⁴⁹ However, these examples offer only limited analogy in support of **13** since the polydentate ligands all alleviate, to at least some extent, the steric problems associated with ligand-ligand interactions within the lithium coordination sphere. It is for this reason that we rephrase the original question more stringently: Is it possible to place five or more discrete ligands around the lithium ion? One structural analogy is particularly compelling. Power and coworkers reported a structure of a coordinatively saturated cobaltate salt bearing a $^+\text{Li}(\text{THF})_5$ counterion (**16**).^{50,51} Although the fifth

(44) Depue, J. S.; Collum, D. B. *J. Am. Chem. Soc.* **1988**, *110*, 5524.

(45) Power, P. P. *Acc. Chem. Res.* **1988**, *21*, 147. Underiner, G.; Tan, R. P.; Powell, D. R.; West, R. *J. Am. Chem. Soc.* **1991**, *113*, 8437. Izatt, R. M.; Pawlak, K.; Bradshaw, J. S.; Bruening, R. L. *Chem. Rev.* **1991**, *91*, 1721. Izatt, R. M.; Bradshaw, R. L.; Nielsen, S. A.; Lamb, J. D.; Christensen, J. J.; Sen, D. *Chem. Rev.* **1985**, *85*, 271.

(46) Li(diamine)₃: Gillier-Pandraud, P. H.; Jamet-Delcroix, S. *Acta Crystallogr., Sect. B* **1971**, *27*, 2476.

(47) For example, $^+\text{Li}(\text{DME})_3$ is octahedral: Niecke, E.; Nieger, M.; Wendroth, P. *Angew. Chem., Int. Ed. Engl.* **1994**, *33*, 353. Niecke, E.; Nieger, M.; Wenderoth, P. *J. Am. Chem. Soc.* **1993**, *115*, 6989. Schumann, H.; Janiak, C.; Pickardt, J. *J. Organomet. Chem.* **1988**, *349*, 117. Bock, H.; Näther, C.; Havlas, Z.; John, A.; Arad, C. *Angew. Chem., Int. Ed. Engl.* **1994**, *33*, 875.

(48) Bürgi, H. B.; Djuric, S.; Dobler, M.; Dunitz, J. D. *Helv. Chim. Acta* **1972**, *55*, 1771. Gentile, P. S.; White, J. G.; Cavalluzzo, D. D. *Inorg. Chim. Acta* **1976**, *20*, 37.

(41) Nicholls, D.; Sutphen, C.; Szwarc, M. *J. Phys. Chem.* **1968**, *72*, 1021. Delsignore, M.; Maaser, H. E.; Petrucci, S. *J. Phys. Chem.* **1984**, *88*, 2405. See also ref 8.

(42) Lucht, B. L.; Collum, D. B. Unpublished.

(43) Ohtaki, H.; Wada, H. *J. Soln. Chem.* **1966**, *70*, 1502. Ohtaki, H. *Pure Appl. Chem.* **1987**, *59*, 1143. Ohtaki, H.; Radnai, T. *Chem. Rev.* **1993**, *93*, 1157.

(axial) THF shows disorder due to partial occupancy, the four other THF ligands clearly define one axial and three equatorial sites of a trigonal bipyramidal coordination sphere. It seems quite reasonable, therefore, to depict the LiHMDS tetrasolvate as trigonal bipyramidal complex **17**.⁵²

Summary and Conclusions

The principle observations and conclusions resulting from this work are as follows:

(1) Dimeric lithium hexamethyldisilazide experiences slow ethereal ligand exchange on NMR time scales. This allows the characterization of mono-, di-, and mixed-solvated dimers (**3**, **1**, and **4**, respectively), the detection of both associative and dissociative ligand substitution pathways (depending on the choice of ligand), determination of relative free energies and enthalpies for solvation by a number of monodentate ethers, and demonstration of non-cooperative mixed solvation.

(2) The different ethereal solvents display a widely varying propensity to cause formation of LiHMDS monomer. The often-cited correlation of reduced aggregation state with increasing strength of the solvent–lithium interaction receives no support whatsoever. The measured free energies of aggregation display a striking solvent dependence that is traced to solvent-independent enthalpies of aggregation and solvent-dependent entropies of aggregation.

(3) LiHMDS monomer is found to be trisolvated rather than disolvated even for fairly hindered ethers. However, the two most strongly coordinating ethers—oxetane and THF—afford considerable concentrations of tetrasolvated monomers assigned as five-coordinate (possibly trigonal bipyramidal). If so, then it would certainly seem likely that monomeric organolithium derivatives in neat THF solutions may routinely retain up to four THF ligands within their coordination spheres.

(4) Overall, the complex relationship between solvation energy and observable aggregation state is understandable only by considering solvent–amide and solvent–solvent interactions on both the monomer and the dimer, the combined contributions of solvation enthalpy and entropy, and the complicating superposition of drifting solvation numbers.

Experimental Section

Reagents and Solvents. All ethers and hydrocarbons were distilled by vacuum transfer from blue or purple solutions containing sodium

(49) Power, P. P.; Xiaojie, X. *J. Chem. Soc., Chem. Commun.* **1984**, 358.

(50) Olmstead, M. M.; Power, P. P.; Sigel, G. *Inorg. Chem.* **1986**, *25*, 1027.

(51) Tetrakis(THF)-solvated lithium ion (⁺Li(THF)₄) is commonly observed crystallographically. See, for example: Eaborn, C.; Hitchcock, P. B.; Smith, J. D.; Sullivan, A. C. *J. Organomet. Chem.* **1984**, *263*, C23.

(52) Sodium ion contains up to six THF ligands: Bock, H.; John, A.; Näther, C.; Havlas, Z.; Mihokova, E. *Helv. Chim. Acta* **1994**, *77*, 41. Jorgensen, W. L.; Chandrasekhar, J. *J. Chem. Phys.* **1982**, *77*, 5080. Gornitzka, H.; Stalke, H. *Angew. Chem., Int. Ed. Engl.* **1994**, *33*, 693.

(53) Kim, Y.-J.; Bernstein, M. P.; Galiano-Roth, A. S.; Romesberg, F. E.; Williard, P. G.; Fuller, D. J.; Harrison, A. T.; Collum, D. B. *J. Org. Chem.* **1991**, *56*, 4435.

(54) Kofron, W. G.; Baclawski, L. M. *J. Org. Chem.* **1976**, *41*, 1879.

(55) Hall, P.; Gilchrist, J. H.; Harrison, A. T.; Fuller, D. J.; Collum, D. B. *J. Am. Chem. Soc.* **1991**, *113*, 9575.

(56) Bax, A.; Griffey, R. H.; Hawkins, B. L. *J. Magn. Reson.* **1983**, *55*, 301. Summers, M. F.; Marzilli, L. G.; Bax, A. *J. Am. Chem. Soc.* **1986**, *108*, 4285.

(57) Bodenhausen, G.; Ruben, D. J. *Chem. Phys. Lett.* **1980**, *69*, 185. Müller, L. *J. Am. Chem. Soc.* **1979**, *101*, 4481.

(58) Stewart, J. J. P. *QCPE* 581.

(59) Clark, T.; Thiel, W. T. *QCPE* 438.

benzophenone ketyl. The hydrocarbon stills contained 1% tetraglyme to dissolve the ketyl. ⁶Li metal (95.5% enriched) was obtained from Oak Ridge National Laboratory. The [⁶Li]ethylolithium used to prepare the ⁶Li labeled LiHMDS was prepared and purified by the standard literature procedure.⁵³ [⁶Li,¹⁵N]LiHMDS was prepared and isolated as an analytically pure solid as described previously.¹¹ The diphenylacetic acid used to check solution titers⁵⁴ was recrystallized from methanol and sublimed at 120 °C under full vacuum. Air and moisture sensitive materials were manipulated under argon or nitrogen using standard glovebox, vacuum line, and syringe techniques.

NMR Spectroscopic Analyses. Samples for spectroscopic analyses were prepared using a sample preparation protocol described in detail elsewhere.^{11,55} Standard ⁶Li, ¹⁵N, and ¹³C NMR spectra were recorded on a Varian XL-400 spectrometer operating at 58.84, 40.52, and 100.58 MHz (respectively) or on a Varian Unity 500 spectrometer operating at 73.57, 58.84, and 125.76 MHz (respectively). The probe temperature was calibrated (±2 °C) by the temperature-dependent chemical shift separation of the two methanol proton resonances using an algorithm provided by Varian. The ⁶Li, ¹⁵N, and ¹³C resonances are referenced to 0.3 M [⁶Li]LiCl/MeOH at −100 °C (0.0 ppm), neat Me₂NEt at −100 °C (25.7 ppm), and the toluene methyl resonance at −100 °C (20.4 ppm), respectively. The ⁶Li–¹⁵N HMQC spectra were recorded on the Varian Unity 500 spectrometer equipped with a custom-built 3-channel probe designed to accommodate lithium and nitrogen pulses with concurrent proton decoupling. The HMQC pulse sequence⁵⁶ was obtained through Varian. The ⁶Li-detected ¹⁵N zero-quantum NMR spectra were recorded using the same spectrometer configuration as for the ⁶Li–¹⁵N HMQC experiments with the following pulse sequence:⁵⁷ 90°_x(⁶Li)–Δ–180°_x(⁶Li)180°_x(¹⁵N)–90°_x(⁶Li)90°_x(¹⁵N) – t₁ –90°_x(⁶Li)90°_φ(¹⁵N)–t₂(⁶Li). Broadband ¹H decoupling was used during all periods of the experiment.²⁵ Data were processed in the phase-sensitive mode.

MNDO Calculations. MNDO calculations were performed on an IBM RISC 6000 cluster using MOPAC⁵⁸ with lithium parameters of Clark and Theil.⁵⁹ All structures were fully optimized under the more rigorous criteria of the keyword PRECISE with no constraints. Each reported heat of formation is the result of a search for the global minimum starting from several different initial geometries. Symmetrical structures were optimized from distorted geometries to ensure that the symmetry is not a calculational artifact. For more sterically crowded systems, the keyword GEO-OK was used with caution to override the small interatomic distance check. These protocols have been applied to other lithium amides as described in detail elsewhere.^{11,30,31}

Acknowledgment. We acknowledge the National Science Foundation Instrumentation Program (CHE 7904825 and PCM 8018643), the National Institutes of Health (RR02002), and IBM for support of the Cornell Nuclear Magnetic Resonance Facility. We thank the National Institutes of Health for direct support of this work and a predoctoral fellowship for B.L.L. We also thank Professors Philip Power and Paul Schleyer as well as colleagues at Cornell for both spirited and helpful discussions.

Note Added in Proof: Manuscripts by G. Hilmersson and O. Davidsson as well as H. J. Reich and co-workers will soon report analogous observations of ethereal solvent in the slow exchange limit.

Supporting Information Available: NMR spectra, computational data, and derivation of eq 12 (32 pages). This material is contained in many libraries on microfiche, immediately follows this article in the microfilm version of the journal, can be ordered from the ACS, and can be downloaded from the Internet; see any current masthead page for ordering information and Internet access instructions.